Dissipation and dilatation rates in premixed turbulent flames

Dissipation and dilatation rates in premixed turbulent flames

V.A. Sabelnikov,[1, a)] A.N. Lipatnikov,[2] S. Nishiki,[3] H. L. Dave,[4] F. E. Hernández Pérez,[5] W. Song,[5] and Hong G. Im[5]

[1)]*Central Aerohydrodynamic Institute (TsAGI), 140180 Zhukovsky, Moscow Region, Russian Federation* [b)]

[2)]*Department of Mechanics and Maritime Sciences, Chalmers University of Technology, Göteborg, 412 96, Sweden*

[3)]*Department of Information and Electronic Engineering, Teikyo University, Utsunomiya 320-8551, Japan*

[4)]*Department of Aerospace Engineering, Indian Institute of Science (IISc), Bengaluru, 560012, India*

[5)]*Clean Combustion Research Center, King Abdullah University of Science and Technology, Thuwal 23955-6900, Saudi Arabia*

(Dated: 7 January 2021)

Velocity dilatation, as well as total, solenoidal, and dilatational dissipation rates of the total flow kinetic energy are extracted from three different direct numerical simulation databases obtained by three independent research groups using different numerical codes and methods (e.g., single-step chemistry and complex chemistry flames) from six different premixed turbulent flames associated with flamelet, thin reaction zone, and broken reaction zone regimes of turbulent burning. Results show that dilatational dissipation can be larger than solenoidal dissipation in the flamelet regime and is substantial in the thin reaction zone regime. Accordingly, the influence of combustion-induced thermal expansion on dissipation rate is not reduced to an increase in the mixture viscosity by the temperature. A simple criterion for identifying conditions associated with significant dilatational dissipation is discussed and dilatational dissipation due to the influence of turbulence on mixing in preheat zones is argued to play a role even at high Karlovitz numbers Ka. In particular, the magnitude of dilatation fluctuations and probability of finding negative local dilatation are increased by Ka, thus, implying that the impact of molecular transport of species and heat on the dilatation increases with increasing Karlovitz number.

PACS numbers: 47.70.Fw, 82.33.Vx, 47.27.-i
Keywords: dissipation rate, solenoidal dissipation, dilatational dissipation, premixed turbulent combustion, thermal expansion, DNS

I. INTRODUCTION

The mean rate $\overline{\rho\varepsilon}$ of viscous dissipation of kinetic energy of a turbulent flow (or dissipation rate for brevity) is one of the most important quantities in the turbulence theory.[1–6] The dissipation rate is defined as follows:

$$\overline{\rho\varepsilon} \equiv \overline{\tau_{ij} S_{ij}}, \tag{1}$$

where

$$\tau_{ij} = 2\mu \left(S_{ij} - \frac{1}{3}\delta_{ij}\frac{\partial u_k}{\partial x_k} \right) + \mu_v \delta_{ij}\frac{\partial u_k}{\partial x_k} \tag{2}$$

is the viscous stress tensor, $S_{ij} = (\partial u_i/\partial x_j + \partial u_j/\partial x_i)/2$ is the strain rate tensor, μ is the dynamic viscosity, μ_v is the bulk viscosity, u_i is the i-th component of the velocity vector $\boldsymbol{u}$, and δ_{ij} is the Kronecker delta, with the summation convention applying to repeated indexes. If $\mu_v = 0$, the dissipation rate can be decomposed as follows:[7–11]

$$\overline{\rho\varepsilon} = \overline{\mu\omega^2} + \frac{4}{3}\overline{\mu\Theta^2} + 2\mu\,\overline{\frac{\partial^2}{\partial x_i \partial x_j}(u_i u_j)} - 4\mu\,\overline{\frac{\partial}{\partial x_i}(u_i\Theta)}, \tag{3}$$

where $\omega^2 = \omega_k\omega_k$ is the enstrophy, $\omega_i = \varepsilon_{ijk}\partial u_j/\partial x_k$ is the i-th component of the vorticity vector, $\Theta = \partial u_k/\partial x_k$ designates dilatation, and ε_{ijk} is the cyclic permutation tensor. The first and second terms on the right hand side (RHS) of Eq. (3) are known as solenoidal and dilatational dissipation,[7] respectively, whereas the third and fourth terms are mixed terms, i.e. they contain contributions from both solenoidal and dilatational velocity components. In the following, these two mixed terms will be considered jointly. If the viscosity μ is constant, the mixed terms asymptotically vanish at high Reynolds numbers because they contain spatial derivatives of mean quantities, whereas the solenoidal and dilatational dissipations involve mean values of squares of local spatial derivatives. For the same reason, dissipation rates evaluated using total or fluctuating velocity fields are asymptotically equal to one another at high Reynolds numbers.

In incompressible turbulent flows, dilatation vanishes and the dissipation rate is asymptotically equal to the solenoidal dissipation at high Reynolds numbers. If density varies due to pressure variations in high-speed flows, heat release at almost constant pressure in low-speed reacting flows, or both pressure variations and heat release (e.g., combustion in supersonic flows), dilatational dissipation plays a role. For instance, in high-speed non-reacting flows, a ratio

$$\chi = \frac{4}{3}\frac{\overline{\Theta^2}}{\overline{\omega^2}} \tag{4}$$

[a)]Electronic mail: sabelnikov@free.fr.
[b)]Also at ONERA - The French Aerospace Lab., F-91761 Palaiseau, France

of dilatational and solenoidal dissipations was reported[7,12] to scale as αM_t^2 in a first approximation, with the factor α being substantially less than unity. Here, $M_t = u'/C$ is the turbulence Mach number, u' is the root-mean-square (rms) velocity, and C is a representative speed of sound. In subsequent studies of compressibility effects on turbulence characteristics (spectra, a ratio of dilatational kinetic energy to solenoidal kinetic energy, a ratio of dilatational dissipation to solenoidal dissipation, etc.) in homogeneous non-reacting flows,[13–18] dependence of the ratio χ on M_t was clarified, e.g. $\chi \propto M_t^4$ at $M_t < 0.4$,[16] with substantial dependence of χ on the turbulent Reynolds number $Re_\lambda = u'\lambda/\nu$ being also documented, as reviewed elsewhere.[17] Here, λ is the Taylor length scale and $\nu = \mu/\rho$ is the kinematic viscosity of the fluid.

Recently, Donzis and John[17] have analyzed a large set of published and their own direct numerical simulation (DNS) data and have shown that the ratio χ is proportional to a ratio of dilatational and solenoidal turbulent kinetic energies, k_d and k_s, respectively, with these two ratios varying by almost ten and five orders of magnitude, respectively. When the same data are plotted vs. M_t, the scatter of the data is significantly more pronounced. More specifically, at $M_t < 0.2$, DNS data generated by Donzis and John[17] using either solenoidal or dilatational forcing differ drastically from one another, i.e., the ratio χ can be as large as 10^3 in the latter case, whereas $\chi \ll 1$ in the former case (if $M_t < 0.2$). An important role played by the ratio of k_d/k_s was also revealed in a recent study of compressibility effects in mixing of passive scalars in homogeneous flows.[18]

In subsonic reacting flows, non-negligible values of the ratio χ were found in non-premixed flames with homogeneous initial conditions at $0 < Ma_t < 0.5$[19–22] and in a spatially developing shear layer at $Ma_t \ll 1$.[23] In all these studies, χ was significantly less than unity. Recently, Teng et al.[16] numerically explored evolution of initially unmixed reacting flows embedded into homogeneous isotropic turbulence. The obtained DNS data show that the ratio χ depends substantially on a heat release parameter (a ratio of the heat of reaction to a reference enthalpy in the cited paper) and a Damköhler number Da, which characterizes a ratio of the turbulence and reaction time scales, whereas the dependence of χ on Re_λ is weakly pronounced at high Da. Under conditions of the discussed DNS, the ratio χ can be larger than unity if $M_t = 0.6$ and the Damköhler number is as large as 3000. However, the computed χ is significantly less than unity for $M_t = 0.2$ even if $Da = 3000$.

Accordingly, to the leading order, the influence of reaction-induced density variations on the dissipation rate may be assumed to be controlled by an increase in the solenoidal dissipation due to an increase in the viscosity with the temperature in reacting flows characterized by a low Mach number.[16,20–22] Contrary to the aforementioned studies of the influence of heat release on dissipation rate in the non-premixed mode of turbulent burning, the present authors are not aware on evaluation of the ratio χ in premixed flames (note that such a flame is characterized by significant spatial gradient of the mean flow velocity in the direction normal to the mean flame surface). Nevertheless, in a recent DNS study[24,25] of highly turbulent premixed flames, the influence of combustion-induced thermal expansion on small-scale turbulence was also attributed to the increase in the mixture viscosity.

Based on the recent findings by Donzis and John,[17] John et al.,[18] and Teng et al.,[16] one may hypothesize that, in premixed turbulent flames characterized by $M_t \ll 1$, the ratio χ depends on Re_λ, k_d/k_s, the density ratio $\sigma = \rho_u/\rho_b$, and Da (note that the Karlovitz number defined later is proportional to Re_λ/Da in premixed flames). In other words, if $M_t \ll 1$,

$$\chi = f(Re_\lambda, k_d/k_s, \sigma, Da), \tag{5}$$

where f is a "universal" non-dimensional function. To our knowledge, there are neither theories nor numerical data on the dependence of the ratio χ on the aforementioned non-dimensional parameters. On the contrary, as reviewed elsewhere,[26,27] numerical modeling of premixed turbulent combustion relies commonly on theories and models of constant-density turbulence characterized by $\nabla \cdot \boldsymbol{u} = 0$ and vanishing dilatational dissipation. Since dissipation rate plays a key role in the turbulence theory,[1–6] eventual change of the physical nature of dissipation in premixed flames when compared to constant-density turbulence, i.e. appearance of dilatational dissipation in the former case, requires thorough investigation and, in particular, evaluation of the ratio χ in the case of premixed turbulent burning.

Accordingly, the major goals of the present study are (i) to examine dilatation in premixed turbulent flames characterized by a very low Mach number and various (small, moderate, and high) Karlovitz numbers and (ii) to demonstrate that dilatational dissipation can play a substantial role in such flames. For this purpose, three DNS databases that are described briefly in the next section were analyzed. Results are reported and discussed in the third section, followed by conclusions.

II. DNS ATTRIBUTES

Analyzed in the present work are the following three DNS databases: (i) Nagoya data that were created by Nishiki et al.[28,29] about 20 years ago and were subsequently explored by various research groups,[30–54] (ii) Bangalore data that were computed recently by Dave and Chaudhuri[55] and were subsequently analyzed by two of the present authors,[56,57] and (iii) KAUST data[58–60] that were also used by various research groups.[61–64] In the following, major attributes of these three DNS series are briefly summarized. The reader interested in more details is referred to the cited papers.

All these unsteady three-dimensional simulations had certain common features. First, they addressed statistically planar and one-dimensional, adiabatic premixed flames propagating in rectangular channels. Second, the governing equations were solved in compressible form. Third, homogeneous isotropic turbulence was generated in a separate box, was injected into the computational domain through the left boundary $x = 0$ and decayed along the direction x of the mean flow. Fourth, the simulated flows were periodic in y and z directions. Fifth, a planar laminar flame was embedded into tur-

bulent flow in the computational domain at $t = 0$. Subsequently, the mean inflow velocity was changed twice[28,29] or gradually[55,58–60] to match turbulent flame speed. Sixth, in the present paper, the combustion progress variable is defined as follows

$$c = \frac{T - T_u}{T_b - T_u}, \tag{6}$$

where T is the temperature and subscripts u and b designate unburned reactants and burned products, respectively.

Major characteristics of the simulated flames are reported in Table I. Here, S_L and $\delta_L = (T_b - T_u)/\max|\nabla T|$ are the laminar flame speed and thickness, respectively, $\sigma = \rho_u/\rho_b$ is the density ratio, u' and L are the rms velocity and an integral length scale, respectively, of turbulence generated in a box, $\tau_t = L/u'$ is the eddy-turn-over time, $Re_t = u'L/\nu_u$ is the turbulent Reynolds number, $Ka = (u'/S_L)^2 Re_t^{-1/2}(S_L\delta_L/\nu_u)$ is the Karlovitz number, and ν_u is the kinematic viscosity of unburned mixture. The Karlovitz number is proportional to a ratio of the flame time scale $\tau_f = \delta_L/S_L$ to the Kolmogorov time scale $\tau_K = (\nu_u/\bar{\varepsilon})^{1/2}$, with the coefficient of proportionality $\sqrt{C_d}$ being of unity order if $\bar{\varepsilon} = C_d u'^3/L$.[2,5] Certain specific features of the discussed DNS databases are noted in the following subsections.

A. Nagoya DNS database

A computational domain of $8 \times 4 \times 4$ mm was resolved using a uniform rectangular ($2\Delta x = \Delta y = \Delta z$) mesh of $512 \times 128 \times 128$ points.

Combustion chemistry was reduced to a single reaction, the Lewis and Prandtl numbers were equal to 1.0 and 0.7, respectively, and the mixture state was completely characterized with a single combustion progress variable c. Temperature-dependence of molecular transport coefficients was taken into account, e.g., $\nu = \nu_u(T/T_u)^{1.7}$.

Flames H and L are characterized by high and low density ratios, respectively, with all other parameters being approximately equal (the first and second lines, respectively, in Table I). These flames are well associated with the flamelet combustion regime,[65] as shown elsewhere.[37]

Results reported in the following were averaged over transverse planes and a time interval of $1.5\tau_t$, associated with fully-developed flames, as discussed in detail elsewhere.[51]

B. Bangalore DNS database

The DNS data were computed adopting the Pencil code.[66] A computational domain of $19.18 \times 4.8 \times 4.8$ mm was discretized using a uniform mesh of $960 \times 240 \times 240$ nodes.

A lean (the equivalence ratio $\Phi = 0.81$) and slightly preheated ($T_u = 310$ K) hydrogen-air flame was studied using a detailed reaction mechanism (9 species, 21 reactions) by Li et al.[67] and mixture-averaged transport coefficients, which depended on temperature. The simulation conditions (flame IIS in the third line in Table I, where IIS is an abbreviation of Indian Institute of Science) are associated with the thin reaction zone regime[65] of turbulent burning.

FIG. 1. Dissipation rate normalized using $\mu_u S_L^2/\delta_L^2$ and various contributions to it vs. Reynolds-averaged combustion progress variable $\bar{c}$. (*a*) Nagoya flame H, (*b*) Nagoya flame L, (*c*) Bangalore flame IIS, (*d*) KAUST flame A, (*e*) KAUST flame B, (*f*) KAUST flame C.

As discussed in detail elsewhere,[56,57] results reported in the following were averaged over transverse planes and various instants (54 snapshots stored each 5 μs over the time period 1.401 ms $\leq t \leq$ 1.566 ms).

C. KAUST DNS database

In cases A and B, a computational domain of $20 \times 10 \times 10$ mm was discretized using a uniform mesh of $512 \times 256 \times 256$ nodes, whereas in case C, a computational domain of $8.32 \times 2.08 \times 2.08$ mm was discretized using a uniform mesh of $1280 \times 320 \times 320$ nodes. To solve the governing equations, an eighth-order central difference and an explicit fourth-order Runge-Kutta schemes were employed.[58]

A lean ($\Phi = 0.70$) hydrogen-air flame ($T_u = 300$ K) was studied using a detailed reaction mechanism (9 species, 19 reactions) by Burke et al.[68] and mixture-averaged transport coefficients, which depended on temperature. The simulation conditions (the three bottom lines in Table I) are associated with flamelet, thin reaction zone, and broken reaction zone regimes[65] of turbulent burning in cases A, B, and C, respectively.

As discussed in detail elsewhere,[63] results reported in the following were averaged over transverse planes and six different instants in each case, i.e., at $t/\tau_t = 0.57$, 0.67, 0.77, 0.86, 0.96, and 1.05 in case A and at $t/\tau_t = 4.1$, 4.8, 5.5, 6.2, 6.8, and 7.5 in cases B and C.

Since the major characteristics of the Nagoya flame H and the KAUST flame A are similar and both flames are associated with flamelet combustion regime, comparison of results computed in these two cases allows us to examine the influence of combustion chemistry and diffusive-thermal effects[69–71] on the dissipation rate. Comparison of results obtained from the Bangalore flame IIS and the KAUST flame B, which both have similar major characteristics and are associated with thin reaction zone regime of turbulent burning, allows us to check the consistency of the two databases. Moreover, comparison of results obtained from the KAUST flames A, B, and C allows us to explore the influence of Karlovitz number on the relation between the dilatational and solenoidal dissipations.

TABLE I. Characteristic parameters of DNS cases

Flame	S_L, m/s	δ_L, mm	σ	u', m/s	L ,mm	τ_t, ms	Re_t	Ka	$Ka/(\sigma-1)$	M_t
H	0.6	0.217	7.53	0.53	3.5	6.6	96	0.60	0.09	0.0015
L	0.416	0.158	2.50	0.53	3.5	6.6	96	0.64	0.43	0.0015
IIS	1.84	0.36	6.15	6.7	3.1	0.46	950	19.0	3.7	0.02
A	1.36	0.36	5.95	0.95	5.0	5.3	227	0.75	0.15	0.002
B	1.36	0.36	5.95	6.8	5.0	0.74	1623	14.4	2.91	0.02
C	1.36	0.36	5.95	19.0	1.4	0.076	1298	126	25.5	0.055

III. RESULTS AND DISCUSSION

A. Comparison of solenoidal and dilatational dissipations

Figure 1 shows the total (solid lines), solenoidal (dashed lines), and dilatational (dotted-dashed lines) dissipations extracted from the six DNS data sets, as well as the sum (double-dashed-dotted lines) of the last two terms on the RHS of Eq. (3), referred to as "mixed." The following trends are worth noting.

First, in all six cases the sum of the last two terms on the RHS of Eq. (3), whether it is positive or negative, is significantly less than the total dissipation, including flames H and L, for which the turbulent Reynolds number is rather small (Figs. 1a and 1b).

Second, for flames H, L, and A in the flamelet combustion regime, the dilatational dissipation can be larger than the solenoidal dissipation. In flame H, characterized by a low Ka and a high density ratio, the ratio χ defined by Eq. (4) is significantly larger than unity in the entire flame brush, with the exception of its trailing zone ($\bar{c} > 0.95$). In flame L, characterized by a comparable Ka, but a significantly lower density ratio, the ratio χ is smaller (larger) than unity at $\bar{c} < 0.4$ ($\bar{c} > 0.4$, respectively). This trend is attributed to decay of the turbulence in the direction of the mean flow and a weak (due to a low density ratio) influence of baroclinic torque on vorticity within the L flame brush.[36] In flame H, such an influence is much stronger, as discussed in detail elsewhere.[36] In flame A characterized by a slightly higher (when compared to flame H) Ka and a lower density ratio, the ratio χ is smaller (larger) than unity at $\bar{c} > 0.4$ ($\bar{c} < 0.4$, respectively). Differences in the behaviour of the ratio χ in flame A compared to flames H/L stem not only from complex-chemistry, but also from diffusive-thermal effects, i.e. significant local variations in the temperature and equivalence ratio due to imbalance of heat and species fluxes from and to reaction zones curved and strained by turbulent eddies. Such effects are well known to play an important role in lean hydrogen-air turbulent flames, as reviewed elsewhere,[69–71] and, in particular, can significantly reduce local burning rate and combustion temperature in negatively curved reaction zones. Since the probability of finding such reaction zones is higher at large $\bar{c}$ due to purely topological reasoning, diffusive-thermal effects could substantially reduce dilatational dissipation at large $\bar{c}$ in lean hydrogen-air turbulent flames.

Third, even in flames IIS and B, characterized by $Ka > 10$ and associated with the thin reaction zone regime of premixed burning, differences between the total and solenoidal dissipations are significant, implying that the dilatational dissipation is not negligible.

Fourth, in flame C, characterized by $Ka > 100$ and associated with the broken reaction zone regime of premixed turbulent burning, the total dissipation is mainly controlled by the solenoidal dissipation. This observation is consistent with recent DNS data that were also obtained from highly turbulent flames.[24,25] Nevertheless, even in this case, dilatational dissipation is substantial at $\bar{c} < 0.1$. Physical mechanisms that could explain this observation will be discussed later. The rapid decrease in $\overline{\rho\varepsilon}$ with $\bar{c}$ observed in Fig. 1f is attributed to turbulence decay due to an increase in the mixture viscosity with increasing temperature.

All in all, Fig. 1 shows that (i) dilatational dissipation can play an important role even at low Mach numbers and (ii) in the flamelet and thin reaction zone regimes of premixed burning, the influence of combustion-induced thermal expansion on dissipation rate is not only due to an increase in the mixture viscosity by the temperature, as commonly believed. Rather, the combustion-induced thermal expansion changes the physical nature of the dissipation, shifting from the dissipation of vortices in constant-density turbulence to the dilatation-controlled dissipation in a premixed flame. Such a fundamental change in the nature of the dissipation in premixed flames casts doubts on the direct application of conventional constant-density turbulence models for simulations of premixed combustion. Other phenomena associated with the influence of combustion-induced thermal expansion on turbulence in premixed flames are reviewed elsewhere.[26,27]

B. A simple criterion to estimate importance of dilatational dissipation

The simplest estimate of a criterion for indicating importance of dilatational dissipation can be obtained by comparing the magnitude of dilatation in the unperturbed laminar flame, i.e. $(\sigma-1)S_L/\delta_L$, with the mean magnitude τ_K^{-1} of velocity gradients generated by the smallest eddies. Accordingly, dilatational dissipation is expected to play a minor role if $Ka/(\sigma-1)$ is significantly larger than unity. As reported in Table I, these values are consistent with the results shown in Fig. 1f. A similar criterion of importance of thermal expansion effects in premixed turbulent flames was earlier proposed by Bilger,[72] but based on a different reasoning. Recent DNS data by MacArt et al.[73,74] are also consistent with such a cri-

terion, while dilatational and solenoidal dissipations are not compared in the cited papers.

Nevertheless, the above simple criterion should be considered with a few cautions. First, it compares a statistically averaged turbulence characteristic, i.e. τ_K^{-1}, with dilatation $(\sigma-1)S_L/\delta_L$ in the local laminar flame. To be more consistent, multiplication of the dilatation with a probability γ of finding such local flames should be used when comparing dilatational and solenoidal dissipations in a premixed turbulent flame. Accordingly, $Ka/(\sigma-1)$ should be compared with $\gamma<1$, rather than unity. Since the probability γ is likely to increase with increasing Ka in moderately turbulent flames and to reach a plateau close to unity at $Ka\gg 1$ and $Da\ll 1$,[75] the actual quantitative criterion is expected to be more complicated.

Second, since combustion increases the mixture viscosity, and hence τ_K, evaluation of this time scale at a temperature higher than T_u, e.g. $(T_u+T_b)/2$, appears to be more consistent. In such a case, $Ka/(\sigma-1)$ should be compared with $\gamma[(1+\sigma)/2]^{0.85}$ if $\nu=\nu_u(T/T_u)^{1.7}$. For typical values of σ, the factor of $\gamma[(1+\sigma)/2]^{0.85}$ could be sufficiently close to unity in the vicinity of the boundary of the domain of importance of dilatational dissipation, but further research into the discussed criterion is definitely required.

Third, in premixed turbulent flames, dilatational dissipation can result not only from heat release, but also from the influence of turbulence on molecular mixing in the local flame zones characterized by a negligible heat release rate. To illustrate such an effect in a simple manner, let us consider the following low-Mach-number transport equation for the temperature[76,78]

$$c_p\rho\frac{\partial T}{\partial t}+c_p\rho u_k\frac{\partial T}{\partial x_k}=c_p\frac{\partial}{\partial t}(\rho T)+c_p\frac{\partial}{\partial x_k}(\rho T u_k)=-\frac{\partial J_{k,T}}{\partial x_k}+\dot{\omega}_T, \quad (7)$$

where c_p is the mixture heat capacity at constant pressure, $\dot{\omega}_T$ is the heat release rate, and the symbol $J_{k,T}$ designates the k-th component of the flux vector $\boldsymbol{J}_T$, which involves fluxes due to molecular transport of heat and species. Using the ideal gas state equation of $pW=\rho RT$ and considering the asymptotic case of a low Mach number $M\ll 1$, which is typical for premixed flames,[76,78] the product of ρT may be substituted with $\rho T=\rho_u T_u[(W/W_u)+O(M^2)]$. Here, W is molecular weight of the mixture and R is the universal gas constant. Accordingly, Eq. (7) reads[78]

$$\Theta\equiv\frac{\partial u_k}{\partial x_k}=\frac{R}{c_p p_u}\left(-\frac{\partial J_{k,T}}{\partial x_k}+\dot{\omega}_T\right)-\frac{1}{W_u}\left(\frac{\partial W}{\partial t}+u_k\frac{\partial W}{\partial x_k}\right). \quad (8)$$

Furthermore, variations in the molecular weight W are weak in a typical premixed flame, where $W\approx W_u$ is controlled by the molecular weight of N_2 to the leading order. Accordingly, the ideal gas state equation is commonly simplified to $\rho T=\rho_u T_u$ in the premixed combustion literature.[76–78] In such a simplified case and if $\boldsymbol{J}_T=-\rho\kappa c_p\nabla T$, Eq. (7) reads[79–81]

$$\Theta=\frac{1}{\rho_u T_u c_p}\left[\frac{\partial}{\partial x_k}\left(\rho\kappa c_p\frac{\partial T}{\partial x_k}\right)+\dot{\omega}_T\right]=\frac{\rho S_d}{\rho_u T_u}|\nabla T|=\frac{\rho(T_b-T_u)}{\rho_u T_u}S_d|\nabla c|, \quad (9)$$

where κ designates molecular heat diffusivity of the mixture and $S_d\equiv[\nabla\cdot(\rho\kappa c_p\nabla T)+\dot{\omega}_T]/(\rho c_p|\nabla T|)$ is a displacement speed[77] of the iso-surface $T(\boldsymbol{x},t)=$const.

Even if time and spatial derivatives of the pressure p and molecular weight W are neglected in Eq. (9), this simplified equation offers an opportunity to illustrate that the local dilatation may be significantly affected by molecular fluxes in preheat (and, to a lesser extent, in radical recombination) zones associated with low reaction rates. Moreover, molecular mixing in turbulent flows is known to be significantly affected by turbulent eddies.[2] Accordingly, at small and large $c(\boldsymbol{x},t)$, the local dilatation could be controlled by turbulence if it is sufficiently strong and the sign of Θ may be not only positive, but also negative (contrary to unperturbed laminar premixed flames where dilatation is always positive). Indeed, in Eq. (9), the dilatation Θ is proportional to the displacement speed S_d, with negative displacements speeds being well documented in DNS studies of highly turbulent premixed flames.[55,82–87] Henceforth, dilatation that stems from the influence of turbulent eddies on molecular mixing in zones where the temperature field is non-uniform due to combustion is called turbulence-controlled dilatation for brevity. Since both this influence and the negative displacement speeds are more pronounced in more intense turbulence, that dilatation could play a substantial role even at a high Karlovitz number and, in particular, could notably affect the dissipation rate. Appearance of zones characterized by negative dilatation and substantial dilatational dissipation is observed upstream of the heat release zone in images plotted in Fig. 2 for the KAUST flames B and, especially C. Certain DNS data that are consistent with this hypothesis are presented in the next subsection.

FIG. 2. Typical 2D images of heat release rate expressed in W/m^3 (top row), normalized dilatation rate $\Theta/[(\sigma-1)S_L/\delta_L]$ (middle row), and normalized dilatational dissipation $4\mu\Theta^2/(3\mu_u S_L^2/\delta_L^2)$ (bottom row, with the color scale being logarithmic) in the KAUST flames A (left column), B (middle column), and C (right columns).

FIG. 3. Probability Density Functions $P(\Theta)$ for the local instantaneous dilatation $\Theta(\boldsymbol{x},t)$ normalized using $(\sigma-1)S_L/\delta_L$ and conditioned to various values of the local instantaneous $c(\boldsymbol{x},t)$, specified in legends. (*a*) Bangalore flame IIS, (*b*) KAUST flame A, (*c*) KAUST flame B, (*d*) KAUST flame C.

C. Influence of Karlovitz number on dilatation

Figure 3 shows variations in the conditioned Probability Density Function (PDF) $P(\Theta^*)$ with the local instantaneous

FIG. 4. Correlation coefficients $C_{a,b} = (\overline{ab} - \bar{a}\bar{b})/(\overline{a'^2}\ \overline{b'^2})^{1/2}$ between dilatation and (*a*) combustion progress variable c, (*b*) strain rate a_t, (*c*) heat release rate $\dot{\omega}_T/c_p$, and (*d*) the magnitude $|\nabla c|$ of the gradient of the combustion progress variable vs. Reynolds-averaged combustion progress variable $\bar{c}$. Abbreviation IIS refers to flame I simulated in the Indian Institute of Science.

combustion progress variable $c(\boldsymbol{x},t)$ that the PDF is conditioned to. These PDFs have been sampled from the entire computational domains in the complex-chemistry cases IIS, A, B, and C. Henceforth, the symbol Θ^* designates the local instantaneous dilatation rate $\Theta(\boldsymbol{x},t)$ normalized using $(\sigma-1)S_L/\delta_L$. The following trends are worth noting.

First, the variations in $P(\Theta^*)$ with $c(\boldsymbol{x},t)$ are non-monotonic. That is, in the upstream region, as $c(\boldsymbol{x},t)$ increases from 0.1 to 0.3, the peak value of the normalized dilatation increases while the PDF distribution broadens (with an exception for case IIS). As $c(\boldsymbol{x},t)$ increases further from 0.3 to 0.7, the PDF distribution becomes narrower while the peak value decreases. This behavior is attributed to the fact that the dilatation and heat release rate peak in the interval of $0.2 < c < 0.3$ in the unperturbed laminar flames associated with the Bangalore and KAUST simulations. Moreover, the monotonic attenuation in turbulence intensity leads to a narrower PDF distribution towards the downstream of the flame.

Second, as expected, the PDFs are wider in more intense turbulence, i.e. at higher Ka, cf. flames A, B, and C.

Third, while the probability of finding negative dilatation is low in flames IIS, A, and B, the PDF $P(\Theta^*)$ does not vanish at negative Θ^* in case C, thus indicating that the turbulence-controlled dilatation does play a role in flame C.

The role of turbulence-controlled dilatation at strong turbulence is further evidenced in Fig. 4, which reports various correlation coefficients $C_{a,b} = (\overline{ab} - \bar{a}\bar{b})/(\overline{a'^2}\ \overline{b'^2})^{1/2}$. In particular, Fig. 4a shows that, in flame H, L, IIS, A, or B, the correlation coefficient $C_{\Theta,c}$ between dilatation and combustion progress variable decreases monotonously with $\bar{c}$ in the largest part of the mean flame brush with the exception of its trailing zones. This trend is associated with the facts that (i) appearance of the local flame in a point $\boldsymbol{x}$ close to the leading (trailing) edge of the mean flame brush causes a positive (negative) local fluctuation $c'(\boldsymbol{x},t)$ and (ii) combustion-induced dilatation is predominantly positive in these weakly and moderately turbulent flames. Accordingly, $C_{\Theta,c}$ is positive at $\bar{c} < c^*$ and negative at $\bar{c} > c^*$, with c^* being close to 0.5. However, such behaviour is not observed in the highly turbulent flame C, where $C_{\Theta,c}$ is close to zero at $\bar{c} < 0.3$, thus implying that other physical mechanisms (e.g. the influence of turbulence on molecular mixing) significantly affect dilatation in that zone. Moreover, in flame C, the coefficient $C_{\Theta,c}$ decreases at $\bar{c} > 0.3$ eventually due to the rapid decay of turbulence, as seen in Fig. 1f. Due to this rapid decay, the turbulence-controlled dilatation effect pronounced in flame C becomes mitigated at $\bar{c} > 0.3$.

Figure 4b shows that the correlation coefficient C_{Θ,a_t} between dilatation and the local strain rate $a_t = -\boldsymbol{nn} : \nabla\boldsymbol{u} + \nabla\cdot\boldsymbol{u}$ is about 0.4-0.5 in the largest parts of the IIS, A, and B flame brushes, as well as in flame C provided that $\bar{c} > 0.3$. Here, $\boldsymbol{n} = -\nabla c/|\nabla c|$ designates the unit normal vector. This positive correlation is attributed to a decrease in the local flame thickness (and, hence, an increase in dilatation) in positively strained local flames. Such an effect is well known in the theory of strained laminar premixed flames[88] since the pioneering work by Klimov.[89] An increase in C_{Θ,a_t} with $\bar{c}$ in the single-step-chemistry flames H and L is attributed to a more important role played by the local curvature (strain rate) at small (large, respectively) $\bar{c}$ in these flames, as discussed elsewhere.[42] However, in the leading zone ($\bar{c} < 0.3$) of flame C, the correlation coefficient is significantly lower than in other complex-chemistry flames, implying again that other physical mechanisms (e.g. the influence of turbulence on molecular mixing) significantly affect dilatation in that zone.

Figure 4c shows that the correlation coefficient C_{Θ,Ω_T} between dilatation and the local heat release rate $\Omega_T = \dot{\omega}_T/c_p$ is close to unity in the largest parts of the IIS, A, and B flame brushes with the exception of their trailing edges, as well as in flame C at $0.6 < \bar{c} < 0.85$. Such a strong correlation implies that the dilatation is mainly controlled by the combustion-induced thermal expansion in these complex-chemistry flames. In the leading zone of the C flame brush, however, the correlation coefficient is lower, again suggesting that other physical mechanisms (e.g. the influence of turbulence on molecular mixing) significantly affect dilatation in that zone. Note that, in the single-step-chemistry flames H and L, the coefficient C_{Θ,Ω_T} is lower, because dilatation and heat release rates peak at significantly different c (0.66 and 0.89, respectively) in the unperturbed laminar flames.

Figure 4d shows that the behaviour of the correlation coefficient $C_{\Theta,|\nabla c|}$ between dilatation and $|\nabla c|$ is similar to the behaviour of C_{Θ,Ω_T}, discussed above. The large value of $C_{\Theta,|\nabla c|}$ results directly from Eq. (9) that shows that $\Theta \propto |\nabla c|$. Lower values of $C_{\Theta,|\nabla c|}$ obtained in the leading zone of flame C indicate that the influence of turbulence on S_d (or, more specifically, on the molecular mixing term in the definition of S_d) plays an important role in that zone, in line with the above discussion of other results reported in Fig. 4. Moreover, these results reveal a way that flame propagation resists to turbulent perturbations, an effect that, to our knowledge, has not yet been discussed in the literature. In other words, if turbulence strongly perturbs a flame locally and makes S_d negative in the flame preheat zone, the turbulence-controlled dilatation increases the local dissipation rate, thus mitigating the local turbulence.

Overall, the present DNS data (in particular, data obtained from flame C) indicate that the turbulence-controlled dilatation may play a role even in highly turbulent flames and, therefore, may notably contribute to the total dissipation rate. This issue definitely requires further DNS research into premixed turbulent flames characterized by Karlovitz numbers higher than the value of $Ka = 126$, which was reached in case C.

Note that if Ka is increased by decreasing the integral length scale L, the mean flame brush thickness δ_t may be decreased. Such an effect is evident in flame C when compared to flames A and B, as discussed elsewhere.[63] In particular, in case C, the time-averaged $\delta_t = 1/\max\{\nabla\bar{c}\}$ (i) is smaller by

FIG. 5. Mean dilatation $\nabla \cdot \bar{\boldsymbol{u}}$ normalized using $(\sigma-1)S_L/\delta_L$ vs. Reynolds-averaged combustion progress variable.

FIG. 6. Magnitude $\overline{(\nabla \cdot \boldsymbol{u}')^2}$ of dilatation fluctuations, normalized using $(\sigma-1)^2 S_L^2/\delta_L^2$, vs. Reynolds-averaged combustion progress variable.

a factor of about 3.5 than in case A or B and (ii) is approximately equal to $3\delta_L$. The decrease in δ_t results in increasing the mean dilatation $\nabla \cdot \bar{\boldsymbol{u}}$. Indeed, Fig. 5 shows that $\nabla \cdot \bar{\boldsymbol{u}}$ is significantly larger in case C when compared to other five cases.

Figure 6 shows that the magnitude $\overline{(\nabla \cdot \boldsymbol{u}')^2}$ of dilatation fluctuations is significantly larger in flame C when compared to other five cases. However, this difference is related more to the turbulence-controlled dilatation rather than to the small thickness δ_t of flame C.

D. Influence of diffusive-thermal effects on dilatation

When analyzing results plotted in Fig. 1f, one might attribute substantial values of dilatational dissipation observed at the leading edge of the mean C flame brush to diffusive-thermal effects, which are discussed in detail elsewhere.[69–71] Such effects are well known to cause significant changes in the local equivalence ratio and enthalpy (when compared to the reference unperturbed laminar flame) due to imbalance of local heat and species fluxes from/to reaction zones wrinkled and strained by turbulent eddies. As a result, in lean hydrogen-air turbulent flames, local reaction rates, $|\nabla c|$, and combustion temperature can be increased if the local flame curvature or strain rate is positive.[88] Consequently, the local dilatation can also be increased.

Such effects are revealed in Fig. 7, which reports PDFs $P(\Theta^*)$ of the normalized dilatation conditioned to various ratios of $\Omega_T(\boldsymbol{x},t)/\max\{\Omega_T(\boldsymbol{x},t)\}$, with the maximum (over the entire computational domain and various instants) heat release rates $\max\{\Omega_T(\boldsymbol{x},t)\}$ being different due to different magnitudes of the diffusive-thermal effects. More specifically, $\max\{\Omega_T(\boldsymbol{x},t)\}$ is significantly increased by Ka, i.e., $\max\{\Omega_T(\boldsymbol{x},t)\} = 8600$, 13 500 and 30 000 (g · K)/(cm^3·s) in flames A, B, and C, respectively. Figure 7 shows that a higher rate $\Omega_T(\boldsymbol{x},t)$ is statistically linked with a higher normalized dilatation Θ^*, with the highest local values of $\Omega_T(\boldsymbol{x},t)$ being accompanied by the highest local values of Θ^*, as for $c = 0.75$ and 0.90. The effect is strongly pronounced in case C, where Θ^* can be as large as 12. Note that an increase in Θ^* from unity to 12 (Fig. 7d) yields an increase in the local dilatational dissipation rate by two orders of magnitude.

FIG. 7. Probability density functions $P(\Theta^*)$ of the normalized dilatation conditioned to various ratios of $\Omega_T(\boldsymbol{x},t)/\max\{\Omega_T(\boldsymbol{x},t)\}$, specified in legends. The PDFs have been sampled from the entire computational domains. (*a*) Bangalore flame IIS, (*b*) KAUST flame A, (*c*) KAUST flame B, (*d*) KAUST flame C.

FIG. 8. (*a*) Probability density functions $P(\delta_L^{-1}\nabla \cdot \boldsymbol{n})$ of the normalized curvature extracted from different zones of the C flame brush, characterized by the mean values of the combustion progress variable specified in legends. (*b*) Variations in the probabilities of $\delta_L^{-1}\nabla \cdot \boldsymbol{n} > 1$ and $\delta_L^{-1}\nabla \cdot \boldsymbol{n} < -1$ in the flame brush.

FIG. 9. Extreme (over transverse plane and time) values of (*a*) local heat release rate normalized using the peak heat release rate in the unperturbed laminar flame and (*b*) normalized dilatation Θ^* vs. mean combustion progress variable. In the right panel, both positive and negative extreme values are plotted using the same line style for each flame, but different colors (red and black, respectively).

Such local perturbations are expected at low values of $\bar{c}$, because positively curved reaction zones are localized at the leading edge of the mean flame brush. Indeed, Fig. 8a shows that the PDF of local curvature $\nabla \cdot \boldsymbol{n}$ normalized using the laminar flame thickness δ_L is shifted to positive values at the leading edge ($\bar{c} = 0.05$) when compared to the middle of the flame brush ($\bar{c} = 0.5$) or its trailing edge ($\bar{c} = 0.95$). As a result, the probability of $\delta_L^{-1}\nabla \cdot \boldsymbol{n}$ being larger than unity is the highest at low $\bar{c}$ and decreases with increasing $\bar{c}$ (Fig. 8b). On the contrary, the probability of $\delta_L^{-1}\nabla \cdot \boldsymbol{n} < -1$ is increased by $\bar{c}$.

While results reported in Figs. 7 and 8 appear to be consistent with the assumption that the diffusive-thermal effects contribute substantially to significant values of dilatational dissipation rate observed in Fig. 1f at small $\bar{c}$, inspection of other DNS data does not support this hypothesis. For instance, Fig. 9 shows that the maximum (over transverse plane and time) values of heat release rate and dilatation (i) depend weakly on the mean combustion progress variable in flames A and B and (ii) peak at values of $\bar{c}$ that are larger than values of $\bar{c}$ associated with the highest dilatational dissipation rate in flame C. The decrease in the extreme values of the normalized Ω_T and Θ^* with the mean combustion progress variable is attributed to the rapid turbulence decay in case C, as seen in Fig. 1f.

Moreover, Fig. 10 indicates that the probability of finding a local heat release rate larger than its maximum value in the unperturbed laminar flame peaks in the middle of the flame brush, rather than at low $\bar{c}$. Furthermore, Fig. 11 shows that a ratio of dilatational and solenoidal dissipation rates (the same rates are plotted in Fig. 1f in another format) does not exhibit a peak at the leading edge of the flame brush in case C, but is increased with $\bar{c}$ up to $\bar{c} \approx 0.8$. This increase can be attributed to the turbulence decay, because the dilatational dissipation rate plays a more important role at lower Ka, as shown in Fig. 1f.

Thus, results reported in Figs. 10 and 11 imply that the sig-

FIG. 10. Probability of finding a local heat release rate larger than its maximum value in the unperturbed laminar flame vs. mean combustion progress variable.

FIG. 11. Ratio of dilatational and solenoidal dissipation rates vs. mean combustion progress variable in flame C.

nificant dilatational dissipation rates encountered at low $\bar{c}$ in case C are unlikely to be caused by the diffusive-thermal effects. Indeed, since the mean thickness of flame C is comparable with the laminar flame thickness ($\delta_t \approx 3\delta_L$), the probability that reaction zones perturbed by turbulent eddies appear at a low $\bar{c}$ is very low. On the contrary, turbulence-controlled dilatation can be observed in preheat zones at a low $\bar{c}$ and a curve plotted in black dotted lines in Fig. 9b does show that the magnitude of negative (turbulence-controlled) dilatation is highest at low $\bar{c}$ in case C. Accordingly, the significant dilatational dissipation rates found at low $\bar{c}$ in case C are associated with the the influence of turbulence on molecular mixing in the preheat zones, rather than with the diffusive-thermal effects. Nevertheless, such effects could play a role in the middle of the flame brush, where (i) the maximum values of the local heat release rate and dilatation are still high (Fig. 9), and (ii) the probability of finding Ω_T larger than its maximum value in the unperturbed laminar flame peaks (Fig. 10). This issue requires further study and will be a subject for future research.

IV. CONCLUSIONS

DNS data obtained by three independent research groups using different numerical codes and methods (e.g., single-step chemistry and complex chemistry flames) from six different premixed turbulent flames associated with flamelet, thin reaction zone, and broken reaction zone regimes of turbulent burning were analyzed to evaluate total, solenoidal, and dilatational dissipations. Results show that dilatational dissipation can be larger than solenoidal dissipation in the flamelet regime and is also significant even in the thin reaction zone regime.

Moreover, certain physical arguments and numerical results imply that dilatational dissipation could play a role even in highly turbulent flames due to the influence of turbulence on molecular mixing in the local flame zones characterized by negligible heat release rate. In particular, due to this physical mechanism, local dilation can be negative and have a large magnitude in the leading zone of the highly turbulent flame C ($Ka > 100$). As a result, a ratio of dilatational and solenoidal dissipations does not vanish in that zone, but stays close to 0.15. Moreover, while local dilatation and heat release rate correlate very well in the complex-chemistry flames IIS, A, and B associated with the flamelet and thin reaction zone regimes of premixed turbulent burning, such a correlation is substantially less pronounced at low $\bar{c}$ in the complex-chemistry flame C characterized by the highest Karlovitz number, thus, indicating again importance of the turbulence-controlled dilatation in that highly turbulent flame.

DNS data obtained from four lean hydrogen-air flames also show that local heat release rate and dilatation can reach values that are significantly (by an order of magnitude in case C) larger than the peak values of these quantities in the unperturbed laminar flames, with the effect magnitudes being increased by Karlovitz number. These findings are attributed to local heating and enrichment of reacting mixture due to imbalance of molecular fluxes of reactants and heat to and from, respectively, reaction zones wrinkled and strained by turbulent eddies. Such effects can also contribute to a substantial role played by dilatational dissipation in premixed turbulent flames.

To our knowledge, the present study provides the first evidence of the importance of dilatational dissipation in premixed turbulent flames characterized by low Mach numbers. In addition, the study shows that the influence of combustion-induced thermal expansion on dissipation rate is not limited to an increase in the mixture viscosity by the temperature.

A substantial role played by dilatational dissipation in premixed turbulent flames casts doubts on the direct application of conventional constant-density turbulence models for simulations of premixed burning. To further investigate dilatation and dilatational dissipation in premixed turbulent flames, a parametric DNS study aimed at exploring the function f on the right hand side of Eq. (5) appears to be of interest. To extend the range of considered parameters, such a study could be performed in the case of a single-step chemistry. Moreover, term-by-term analysis of the exact equation for dilatation appears to be of interest also and will be the subject of future work.

ACKNOWLEDGMENTS

The authors are grateful to Prof. Chaudhuri for his valuable contribution to the DNS of flame IIS. VAS gratefully acknowledges the financial support by the Grant of the Ministry of Education and Science of the Russian Federation (Contract No. 14.G39.31.0001 of February 13, 2017). ANL gratefully acknowledges the financial support by the Combustion Engine Research Center (CERC). HLD acknowledges the computational resources provided by the Supercomputer Education and Research Centre (SERC), IISc for performing the DNS calculation (flame IIS). WS, FEHP, and HGI were sponsored by King Abdullah University of Science and Technology (KAUST). Computational resources for the DNSs of flames A, B, and C were provided by the KAUST Supercomputing Laboratory.

Data availability statement

The data that support the findings of this study are available from the corresponding author upon reasonable request.

[1] A. N. Kolmogorov, "The local structure of turbulence in incompressible viscous fluid for very large Reynolds number," Dokl. Akad. Nauk SSSR **30**, 299 (1941).
[2] A. S. Monin and A. M. Yaglom, *Statistical Fluid Mechanics: Mechanics of Turbulence*, vol. 2 (The MIT Press, Cambridge, Massachusetts, 1975).
[3] L. D. Landau and E. M. Lifshitz, *Fluid Mechanics* (Pergamon Press, Oxford, UK, 1987).
[4] U. Frisch, *Turbulence: The Legacy of A.N. Kolmogorov* (Cambridge University Press, Cambridge, UK, 1995).

[5]S. B. Pope, *Turbulent Flows* (Cambridge University Press, Cambridge, UK, 2000).
[6]A. Tsinober, *An Informal Conceptual Introduction to Turbulence* (Springer, Heidelberg, Germany, 2009).
[7]S. K. Lele, "Compressibility effects on turbulence," Annu. Rev. Fluid Mech. **26**, 211 (1994).
[8]P. G. Huang, G. N. Coleman, and P. Bradshow, "Compressible turbulence channel flows: DNS results and modeling," J. Fluid Mech. **305**, 185 (1995).
[9]V. M. Canuto, "Compressible turbulence," Astr. J. **482**, 827 (1997).
[10]R. Friedrich and F. P. Bertolloti, "Compressibility effects due to turbulence fluctuations," Appl. Sci. Res. **57**, 165 (1997).
[11]Y. Andreopoulos, J. H. Agui, and G. Briassulis, "Shock wave-turbulence interactions," Annu. Rev. Fluid. Mech. **32**, 309 (2000).
[12]O. Zeman, "Dilatation dissipation: the concept and application in modeling compressible mixing layers," Phys. Fluids A **2**, 78 (1990).
[13]S. Jagannathan and D. A. Donzis, "Reynolds and Mach number scaling in solenoidally-forced compressible turbulence using high-resolution direct numerical simulations," J. Fluid Mech. **789**, 669 (2016).
[14]J. Wang, T. Gotoh, and T. Watanabe, "Spectra and statistics in compressible isotropic turbulence," Phys. Rev. Fluids **2**, 013403 (2017).
[15]J. P. John, D. A. Donzis, and K. R. Sreenivasan, "Solenoidal scaling laws for compressible mixing," Phys. Rev. Lett. **123**, 224501 (2019).
[16]J. Teng, J. Wang, H. Li, and S. Chen, "Spectra and scaling in chemically reacting compressible isotropic turbulence," Phys. Rev. Fluids **5**, 084601 (2020).
[17]D. A. Donzis and J. P. John, "Universality and scaling in homogeneous compressible turbulence," Phys. Rev. Fluids **5**, 084609, (2020).
[18]J. P. John, D. A. Donzis, and K. R. Sreenivasan, "Compressibility effects on the scalar dissipation rate," Combust. Sci. Technol. **192**, 1320 (2020).
[19]F. A. Jaberi and C. K. Madnia, "Effects of heat of reaction on homogeneous compressible turbulence," J. Sci. Computing **13**, 201 (1998).
[20]M. P. Martín and G. Candler, "Effect of chemical reactions on decaying isotropic turbulence," Phys. Fluids **10**, 1715 (1998).
[21]F. A. Jaberi, D. Livescu, and C. K. Madnia, "Characteristics of chemically reacting compressible homogeneous turbulence," Phys. Fluids **12**, 1189 (2000).
[22]D. Livescu, F. A. Jaberi, and C. K. Madnia, "The effects of heat release on the energy exchange in reacting turbulent shear flow," J. Fluid Mech. **450**, 35 (2002).
[23]S. D. Mason and C. J. Rutland, "Turbulent transport in spatially developing reacting shear layers," Proc. Combust. Inst. **28**, 505 (2000).
[24]B. Bobbitt and G. Blanquart, "Vorticity isotropy in high Karlovitz number premixed flames flames," Phys. Fluids **28**, 105101 (2016).
[25]B. Bobbitt, S. Lapointe, and G. Blanquart, "Vorticity transformation in high Karlovitz number premixed flames," Phys. Fluids **28**, 015101 (2016).
[26]A. N. Lipatnikov and J. Chomiak, "Effects of premixed flames on turbulence and turbulent scalar transport," Prog. Energy Combust. Sci. **36**, 1 (2010).
[27]V. A. Sabelnikov and A. N. Lipatnikov, "Recent advances in understanding of thermal expansion effects in premixed turbulent flames," Annu. Rev. Fluid Mech. **49**, 91 (2017).
[28]S. Nishiki, T. Hasegawa, R. Borghi, and R. Himeno, "Modeling of flame-generated turbulence based on direct numerical simulation databases," Proc. Combust. Inst. **29**, 2017 (2002).
[29]S. Nishiki, T. Hasegawa, R. Borghi, and R. Himeno, "Modelling of turbulent scalar flux in turbulent premixed flames based on DNS databases," Combust. Theory Modelling **10**, 39 (2006).
[30]Y. H. Im, K. Y. Huh, S. Nishiki, and T. Hasegawa, "Zone conditional assessment of flame-generated turbulence with DNS database of a turbulent premixed flame," Combust. Flame **137**, 478 (2004).
[31]A. Mura, K. Tsuboi, and T. Hasegawa, "Modelling of the correlation between velocity and reactive scalar gradients in turbulent premixed flames based on DNS data," Combust. Theory Modelling **12**, 671 (2008).
[32]A. Mura, V. Robin, M. Champion, and T. Hasegawa, "Small scale features of velocity and scalar fields in turbulent premixed flames," Flow Turbul. Combust. **82**, 339 (2009).
[33]V. Robin, A. Mura, M. Champion, and T. Hasegawa, "Direct and indirect thermal expansion effects in turbulent premixed flames," Combust. Sci. Technol. **182**, 449 (2010).
[34]V. Robin, A. Mura, and M. Champion, "Modeling of the effects of thermal expansion on scalar turbulent fluxes in turbulent premixed flames," J. Fluid Mech. **689**, 149 (2011).
[35]K. N. C. Bray, M. Champion, P. A. Libby, and N. Swaminathan, "Scalar dissipation and mean reaction rates in premixed turbulent combustion," Combust. Flame **158**, 2017 (2011).
[36]A. N. Lipatnikov, S. Nishiki, and T. Hasegawa, "A direct numerical simulation study of vorticity transformation in weakly turbulent premixed flames," Phys. Fluids **26**, 105104 (2014).
[37]A. N. Lipatnikov, S. Nishiki, and T. Hasegawa, "DNS assessment of relation between mean reaction and scalar dissipation rates in the flamelet regime of premixed turbulent combustion," Combust. Theory Modell. **19**, 309 (2015).
[38]A. N. Lipatnikov, J. Chomiak, V. A. Sabelnikov, S. Nishiki, and T. Hasegawa, "Unburned mixture fingers in premixed turbulent flames," Proc. Combust. Inst. **35**, 1401 (2015).
[39]A. N. Lipatnikov, V. A. Sabelnikov, S. Nishiki, T. Hasegawa, and N. Chakraborty, "DNS assessment of a simple model for evaluating velocity conditioned to unburned gas in premixed turbulent flames," Flow Turbul. Combust. **94**, 513 (2015).
[40]V. A. Sabelnikov, A. N. Lipatnikov, N. Chakraborty, S. Nishiki, and T. Hasegawa, "A transport equation for reaction rate in turbulent flows," Phys. Fluids **28**, 081701 (2016).
[41]V. A. Sabelnikov, A. N. Lipatnikov, N. Chakraborty, S. Nishiki, and T. Hasegawa, "A balance equation for the mean rate of product creation in premixed turbulent flames," Proc. Combust. Inst. **36**, 1893 (2017).
[42]A. N. Lipatnikov, V. A. Sabelnikov, S. Nishiki, and T. Hasegawa, "Flamelet perturbations and flame surface density transport in weakly turbulent premixed combustion," Combust. Theory Modell. **21**, 205 (2017).
[43]A. N. Lipatnikov, J. Chomiak, V. A. Sabelnikov, S. Nishiki, and T. Hasegawa, "A DNS study of the physical mechanisms associated with density ratio influence on turbulent burning velocity in premixed flames," Combust. Theory Modell. **22**, 131 (2018).
[44]A. N. Lipatnikov, V. A. Sabelnikov, N. Chakraborty, S. Nishiki, and T. Hasegawa, "A DNS study of closure relations for convection flux term in transport equation for mean reaction rate in turbulent flow," Flow Turbul. Combust. **100**, 75 (2018).
[45]A. N. Lipatnikov, V. A. Sabelnikov, S. Nishiki, and T. Hasegawa, "Combustion-induced local shear layers within premixed flamelets in weakly turbulent flows," Phys. Fluids **30**, 085101 (2018).
[46]A. N. Lipatnikov, V. A. Sabelnikov, S. Nishiki, and T. Hasegawa, "Does flame-generated vorticity increase turbulent burning velocity?" Phys. Fluids **30**, 081702 (2018).
[47]A. N. Lipatnikov, S. Nishiki, and T. Hasegawa, "A DNS assessment of linear relations between filtered reaction rate, flame surface density, and scalar dissipation rate in a weakly turbulent premixed flame," Combust. Theory Modell. **23**, 245 (2019).
[48]A. N. Lipatnikov, S. Nishiki, and T. Hasegawa, "Closure relations for fluxes of flame surface density and scalar dissipation rate in turbulent premixed flames," Fluids **4**, 43 (2019).
[49]A. N. Lipatnikov, V. A. Sabelnikov, S. Nishiki, and T. Hasegawa, "A direct numerical simulation study of the influence of flame-generated vorticity on reaction-zone-surface area in weakly turbulent premixed combustion," Phys. Fluids **31**, 055101 (2019).
[50]V. A. Sabelnikov, A. N. Lipatnikov, S. Nishiki, and T. Hasegawa, "Application of conditioned structure functions to exploring influence of premixed combustion on two-point turbulence statistics," Proc. Combust. Inst. **37**, 2433 (2019).
[51]V. A. Sabelnikov, A. N. Lipatnikov, S. Nishiki, and T. Hasegawa, "Investigation of the influence of combustion-induced thermal expansion on two-point turbulence statistics using conditioned structure functions," J. Fluid Mech. **867**, 45 (2019).
[52]V. A. Sabelnikov, A. N. Lipatnikov, N. Nikitin, S. Nishiki, and T. Hasegawa, "Application of Helmholtz-Hodge decomposition and conditioned structure functions to exploring influence of premixed combustion on turbulence upstream of the flame," Proc. Combust. Inst. **38**, https://doi.org/10.1016/j.proci.2020.09.015.
[53]V. A. Sabelnikov, A. N. Lipatnikov, N. Nikitin, S. Nishiki, and T. Hasegawa, "Solenoidal and potential velocity fields in weakly turbulent premixed flames," Proc. Combust. Inst. **38**, https://doi.org/10.1016/j.proci.2020.09.016.

[54] A. N. Lipatnikov, V. A. Sabelnikov, S. Nishiki, and T. Hasegawa, "Influence of thermal expansion on potential and rotational components of turbulent velocity field within and upstream of premixed flame brush," Flow Turbul. Combust. https://doi.org/10.1007/s10494-020-00131-3.

[55] H. Dave and S. Chaudhuri, "Evolution of local flame displacement speeds in turbulence," J. Fluid Mech. **884**, A46 (2020).

[56] A. N. Lipatnikov and V. A. Sabelnikov, "An extended flamelet-based presumed probability density function for predicting mean concentrations of various species in premixed turbulent flames," Int. J. Hydrogen Energy **45**, 31162 (2020).

[57] A. N. Lipatnikov and V. A. Sabelnikov, "Evaluation of mean species mass fractions in premixed turbulent flames: A DNS study," Proc. Combust. Inst. **38**, https://doi.org/10.1016/j.proci.2020.05.006.

[58] H. G. Im, P. G. Arias, S. Chaudhuri, and H. A. Uranakara, "Direct numerical simulations of statistically stationary turbulent premixed flames," Combust. Sci. Technol. **188**, 1182 (2016).

[59] H. A. Uranakara, S. Chaudhuri, H. L. Dave, P. G. Arias, and H. G. Im, "A flame particle tracking analysis of turbulence-chemistry interaction in hydrogen-air premixed flames," Combust. Flame **163**, 220 (2016).

[60] D. H. Wacks, N. Chakraborty, M. Klein, P. G. Arias, and H. G. Im, "Flow topologies in different regimes of premixed turbulent combustion: A direct numerical simulation analysis," Phys. Rev. Fluids **1**, 083401 (2016).

[61] M. Klein, A. Herbert, H. Kosaka, B. Böhm, A. Dreizler, N. Chakraborty, V. Papapostolou, H. G. Im, and J. Hasslberger, "Evaluation of flame area based on detailed chemistry DNS of premixed turbulent hydrogen-air flames in different regimes of combustion," Flow Turbul. Combust. **104**, 403 (2020).

[62] D. M. Manias, E. Al. Tingas, F. E. Hernández-Pérez, R. M. Galassi, P. P. Ciottoli, M. Valorani, and H. G. Im, "Investigation of the turbulent flame structure and topology at different Karlovitz numbers using the tangential stretching rate index," Combust. Flame **200**, 155 (2019).

[63] A. N. Lipatnikov, V. A. Sabelnikov, F. E. Hernández-Pérez, W. Song, and H. G. Im, "A priori DNS study of applicability of flamelet concept to predicting mean concentrations of species in turbulent premixed flames at various Karlovitz numbers," Combust. Flame **222**, 370 (2020).

[64] A. N. Lipatnikov, V. A. Sabelnikov, F. E. Hernández-Pérez, W. Song, and H. G. Im, "Prediction of mean radical concentrations in lean hydrogen-air turbulent flames at different Karlovitz numbers adopting a newly extended, flamelet-based presumed PDF," Combust. Flame **226**, 248 (2021).

[65] N. Peters, "The turbulent burning velocity for large-scale and small-scale turbulence," J. Fluid Mech. **384**, 107 (1999).

[66] N. Babkovskaia, N. E. L. Haugen, and A. Brandenburg, "A high-order public domain code for direct numerical simulations of turbulent combustion," J. Comput. Phys. **230**, 1 (2011).

[67] J. Li, Z. Zhao, A. Kazakov, and F. L. Dryer, "An updated comprehensive kinetic model of hydrogen combustion," Int. J. Chem. Kinetics **36**, 566 (2004).

[68] M. P. Burke, M. Chaos, Y. Ju, F. L. Dryer, and S. J. Klippenstein, "Comprehensive H_2/O_2 kinetic model for high-pressure combustion," Int. J. Chem. Kinet. **44**, 444 (2012).

[69] V. R. Kuznetsov and V. A. Sabelnikov, *Turbulence and Combustion* (Hemisphere Publ. Corp., New York, 1990).

[70] A. N. Lipatnikov and J. Chomiak, "Molecular transport effects on turbulent flame propagation and structure," Prog. Energy Combust. Sci. **31**, 1 (2005).

[71] A. Lipatnikov, *Fundamentals of Premixed Turbulent Combustion* (CRC Press, Boca Raton, Florida, 2012).

[72] R. W. Bilger, "Some aspects of scalar dissipation," Flow Turbul. Combust. **72**, 93 (2004).

[73] J. F. MacArt, T. Grenga, and M. E. Mueller, "Effects of combustion heat release on velocity and scalar statistics in turbulent premixed jet flames at low and high Karlovitz numbers," Combust. Flame **191**, 468 (2018).

[74] J. F. MacArt, T. Grenga, and M. E. Mueller, "Evolution of flame-conditioned velocity statistics in turbulent premixed jet flames at varying Karlovitz number," Proc. Combust. Inst. **37**, 2503 (2019).

[75] V. A. Sabelnikov, R. Yu, and A. N. Lipatnikov, "Thin reaction zones in constant-density turbulent flows at low Damköhler numbers: Theory and simulations," Phys.Fluids **31**, 055104 (2019).

[76] Ya. B. Zel'dovich, G. I. Barenblatt, V. B. Librovich, and G. M. Makhviladze, *The Mathematical Theory of Combustion and Explosions* (Consultants Burea, New York, 1985).

[77] N. Peters, *Turbulent Combustion* (Cambridge University Press, Cambridge, UK, 2000).

[78] T. Poinsot and D. Veynante, *Theoretical and Numerical Combustion*, second ed. (Edwards, Philadelphia, 2005).

[79] A. G. Prudnikov, "Burning of homogeneous fuel-air mixtures in a turbulent flow," in *Physica Principles of the Working Process in Combustion Chambers of Jet Engines*, edited by B. V. Raushenbakh (Clearing House for Federal Scientific & Technical Information, Springfield, 1967), pp. 244-336.

[80] N. Chakraborty and R. S. Cant, "Influence of Lewis number on curvature effects in turbulent premixed flame propagation in the thin reaction zone regime," Phys. Fluids **17**, 105105 (2005).

[81] G. Troiani, F. Battista, and F. Picano, "Turbulent consumption speed via local dilatation rate measurements in a premixed bunsen jet," Combust. Flame **160**, 2029 (2013).

[82] I. Gran, T. Echekki, and J. H. Chen, "Negative flame speed in an unsteady 2-D premixed flame: a computational study," Proc. Combust. Inst. **26**, 323 (1996).

[83] N. Peters, P. Terhoeven, J. H. Chen, and T. Echekki, "Statistics of flame displacement speeds from computations of 2-D unsteady methane-air flames," Proc. Combust. Inst. **27**, 833 (1998).

[84] N. Chakraborty, M. Klein, and R. S. Cant, "Stretch rate effects on displacement speed in turbulent premixed flame kernels in the thin reaction zone regime," Proc. Combust. Inst. **31**, 1385 (2007).

[85] H. Wang, E. R. Hawkes, and J. H. Chen, "A direct numerical simulation study of flame structure and stabilization of an experimental high Ka CH_4/air premixed jet flame," Combust. Flame **180**, 110 (2017).

[86] S. Luca, A. Attili, E. L. Schiavo, F. Creta, and F. Bisetti, "On the statistics of flame stretch in turbulent premixed jet flames in the thin reaction zone regime at varying Reynolds number," Proc. Combust. Inst. **37**, 2451 (2019).

[87] R. Yu, T. Nilsson, C. Fureby, and A. Lipatnikov, "Evolution equations for the decomposed components of displacement speed in a reactive scalar field," J. Fluid Mech., in press.

[88] P. Clavin, "Dynamical behavior of premixed flame fronts in laminar and turbulent flows," Prog. Energy Combust. Sci. **11**, 1 (1985).

[89] A. M. Klimov, "Laminar flame in a turbulent flow," Zh. Prikl. Mekch. Tekhn. Fiz. **4**, No. 3, 49 (1963).

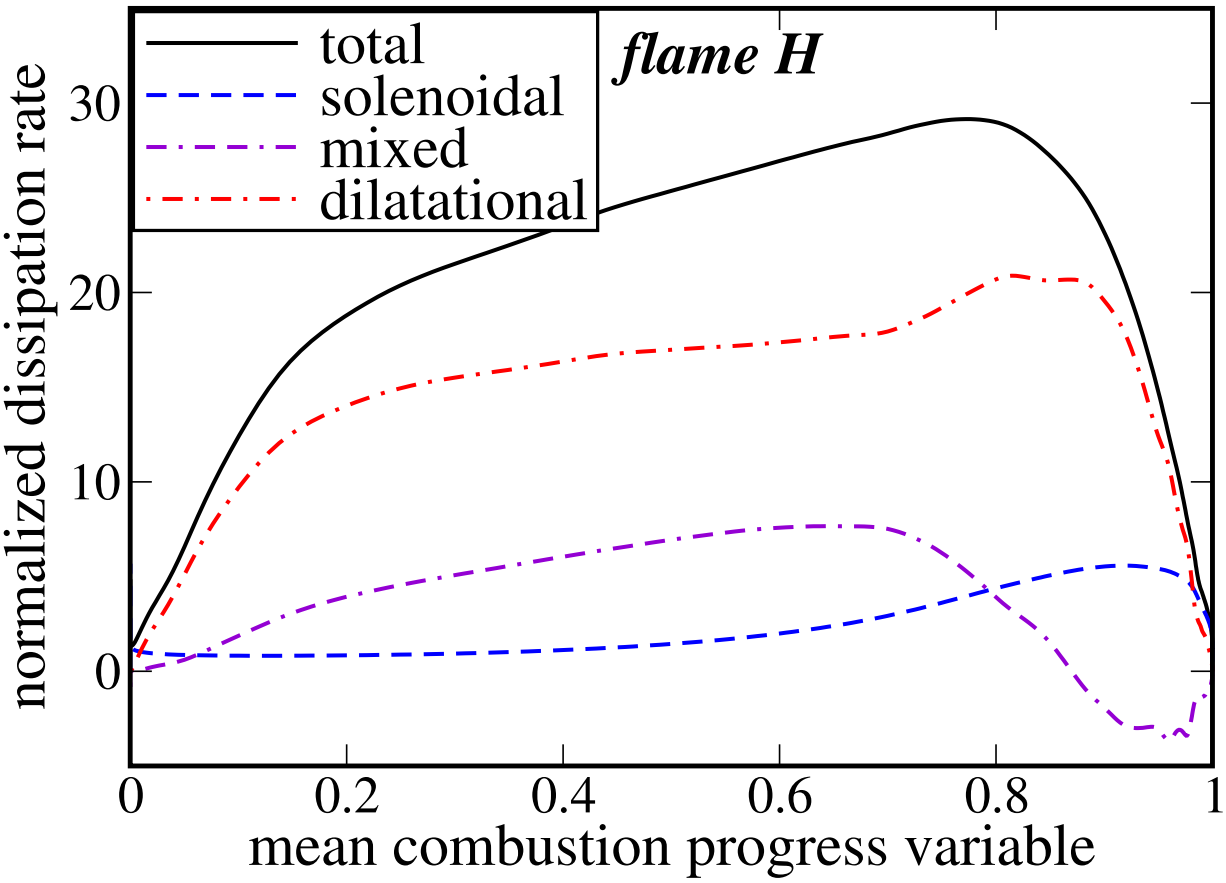

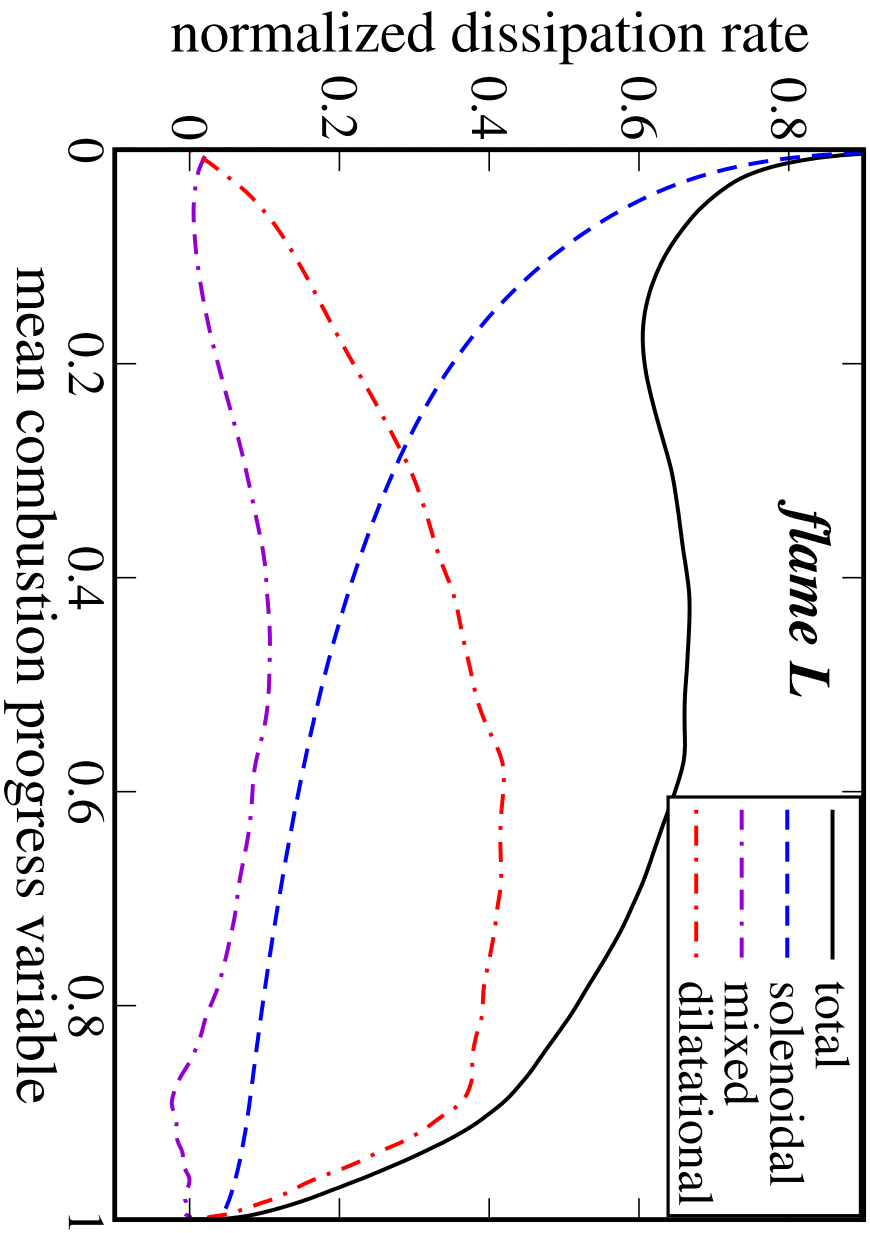

PLEASE CITE THIS ARTICLE AS DOI: 10.1063/5.0039101

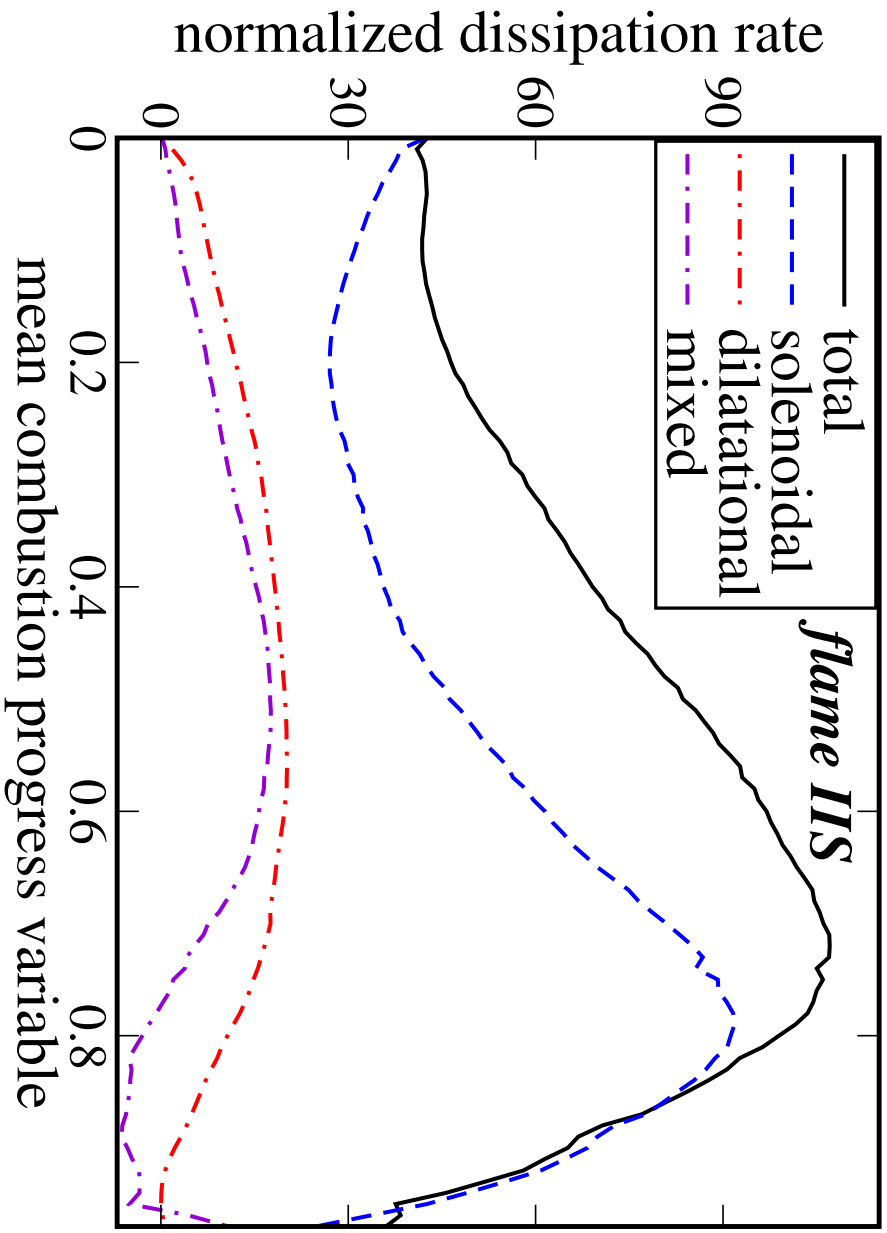

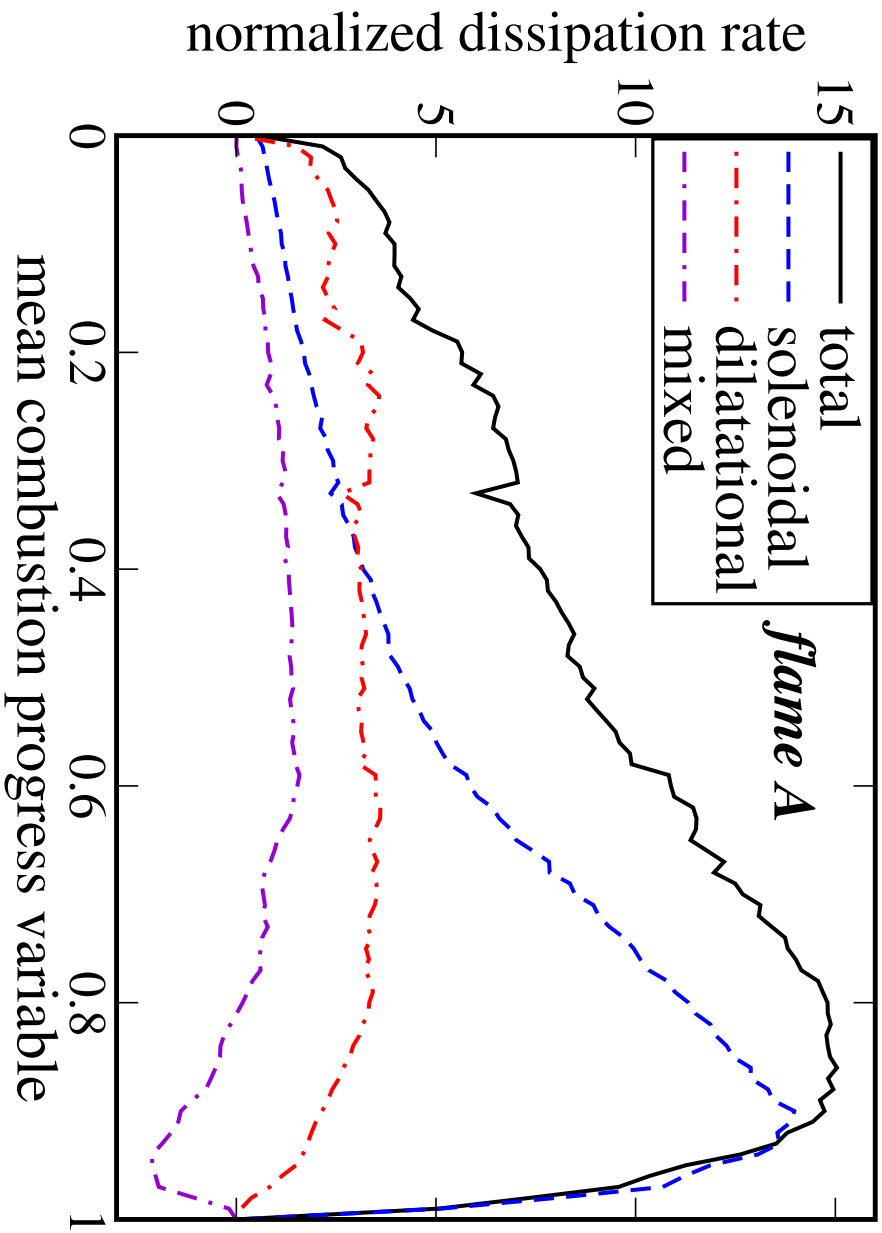

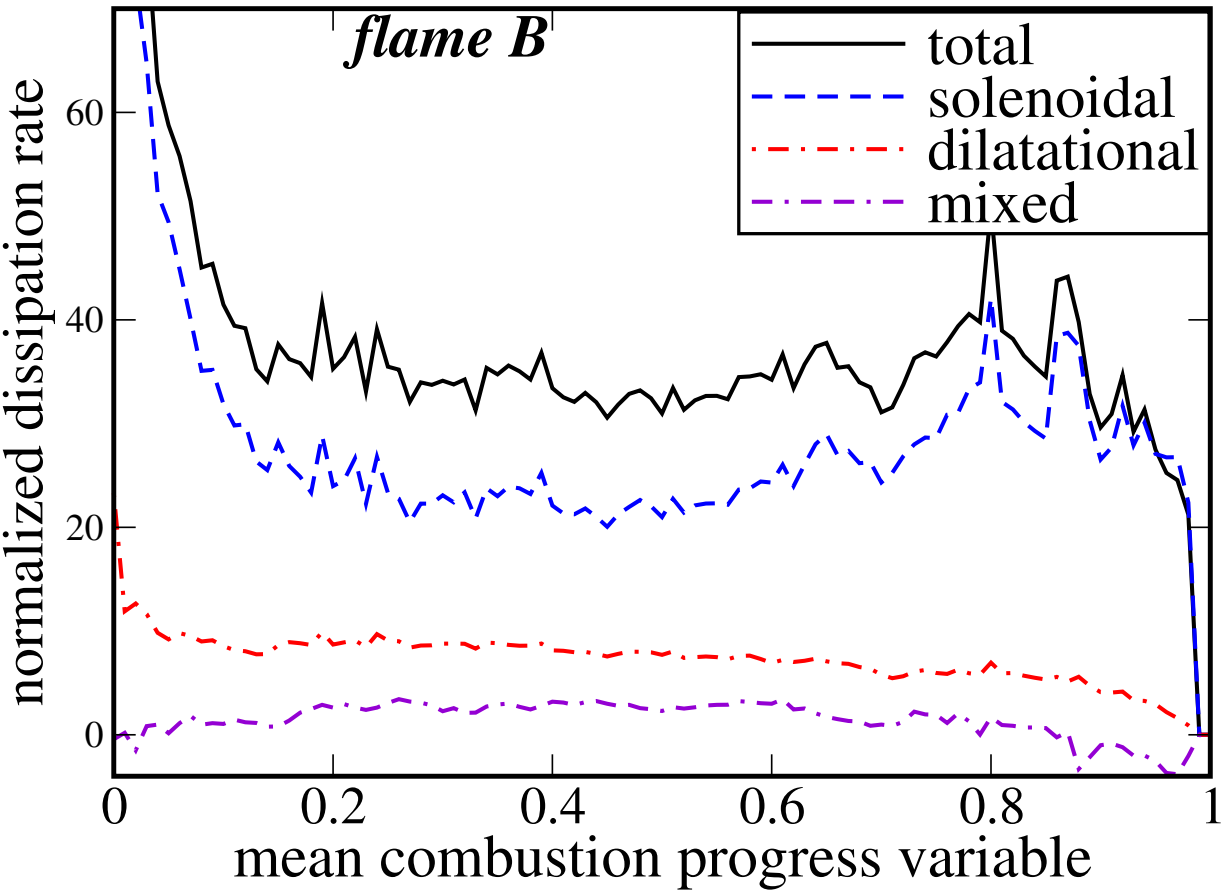

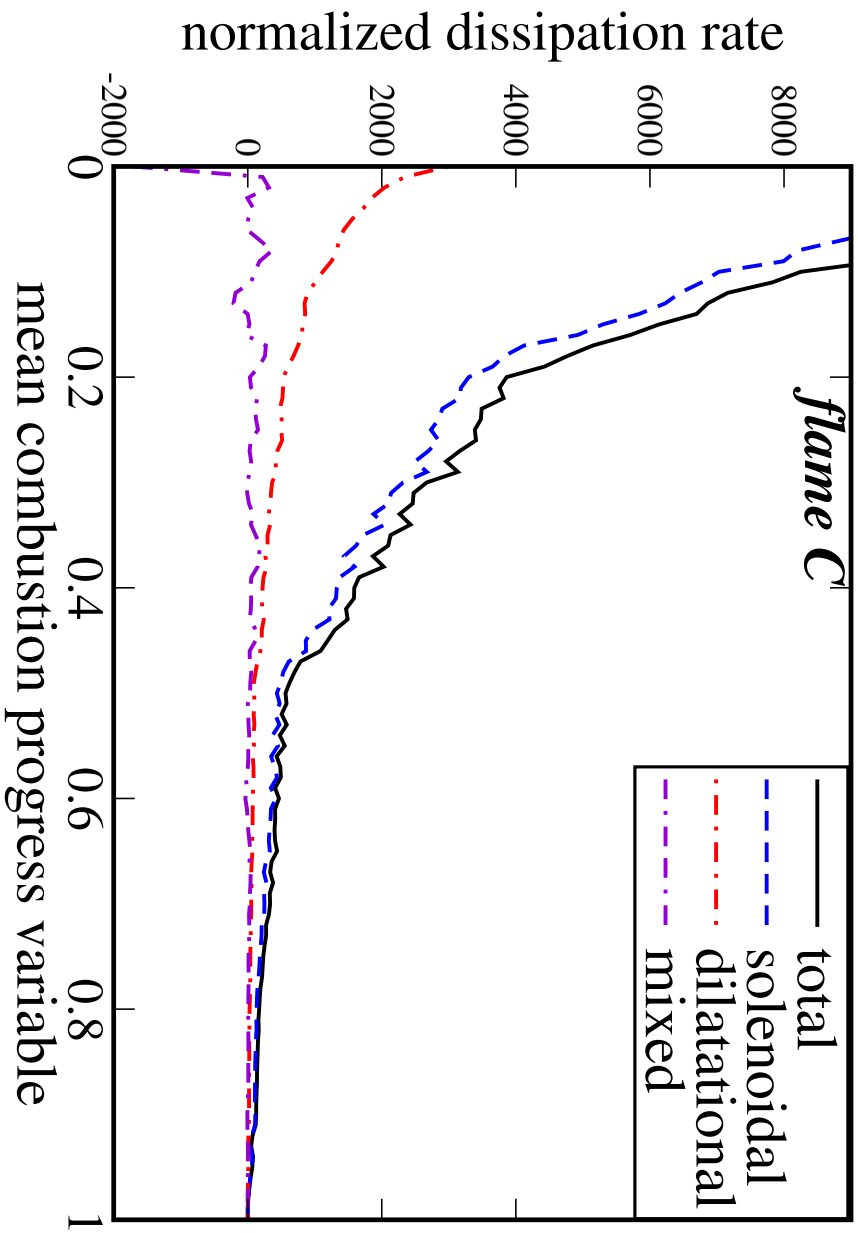

PLEASE CITE THIS ARTICLE AS DOI: 10.1063/5.0039101